APEM journal
Advances in Production Engineering & Management
Volume 10 | Number 2 | June 2015 | pp 97–107
http://dx.doi.org/10.14743/apem2015.2.195
ISSN 1854-6250
Journal home: apem-journal.org
Original scientific paper

Wear characteristics of heat-treated Hadfield austenitic manganese steel for engineering application

Agunsoye, J.O.[a,*], **Talabi, S.I.**[b], **Bello, O.**[a]

[a]Department of Metallurgical and Materials Engineering, University of Lagos, Akoka, Nigeria
[b]Department of Materials and Metallurgical Engineering, University of Ilorin, Ilorin, Nigeria

ABSTRACT

The wear behaviour was investigated of heat treated Hadfield austenitic manganese steel (HAMnS). The wear test was carried out using spin on disc apparatus under different loading loads and speed conditions. A scanning electron microscopy (SEM), an X-ray diffractometer and micro-hardness testing machines were used for examining the morphology, compositions and to measure the hardness of the manganese steel, respectively. The results of the wear test showed that the sliding speed-time interactions effect gave the most significant effect on the austenitic manganese steel. The solution heat treatment programme increased the wear resistance of the alloy steel under increasing load, speed and time. The as-cast microstructure was characterized by heterogeneously dispersed chromium carbides second phase particle, and was responsible for the observed non-uniform wear rate. In regard to the solution heat treated HAMnS, the segregated carbides were dissolved at 1050 °C and uniformly dispersed within the matrix of its microstructure after rapid water quenching to room temperature. This later development was responsible for the uniform and improved wear resistance of the manganese steel casting. This work demonstrated significantly that there is a direct relationship between the second phase carbides, their distribution and the wear rate pattern of HAMnS casting.

ARTICLE INFO

Keywords:
Manganese steel
Wear behaviour
Solution heat treatment
Microstructure
Hardness

**Corresponding author:*
jagunsoye@unilag.edu.ng
(Agunsoye, J.O.)

Article history:
Received 18 November 2014
Revised 30 March 2015
Accepted 7 April 2015

1. Introduction

A lot of money has been spent on using electricity and explosive to break rocks. The motivation to reduce energy consumption has led to the use of non-explosive means to break rocks and extract valuable minerals [1]. The non-explosive means has advantage of avoiding sudden removal of plastic-elastic energy that can cause fracture by blasting. But due to wear, the materials used in breaking this rocks usually required early replacement. The replacement of item involves both material and manpower cost. There are different kinds of wear-resistant materials that are used for processing of solid mineral vis-a-vis crushing and grinding. The traditional materials include wear resistance high chromium iron, hyper-steel, medium carbon steel that are case-hardened, manganese steel etc. In general terms, the high chromium iron suitable for wear resisting applications fall within the compositional limits bounded by the austenitic phase field of the ternary liquidus surface of the iron, chromium, carbon diagram [2]. However the use of high chromium wear resistant iron comes at a huge cost. The material is also known to be characteristically very hard and brittle. Consequently this grade of material is prone to crack under repeated impact load in areas where impact is common [3]. They are usually used in the quarry as

cast plate for bottom liners and as side plate for crushing of hard solid minerals. Regrettably once they are broken, there is no possibility of salvage through hard-facing with wear resistance electrodes. Because of the frequent breakage of high chromium resistant iron, there is a need for the development of a wear-resistant alloy steel that will have high wear resistant, tough and hard at the same time. So in 1882, austenitic manganese rich steel (Hadfield steel), containing between 11 % and 14 % manganese and about 1.2 % carbon, was developed about 13 decades ago and its consequent use for high-wear applications [4]. Major advantages of this material include its toughness and ductility, and the fact that continuous surface impacts result in work-hardening without any increase in brittleness. Consequently, Hadfield steels and their technological descendants provide both strength and abrasion resistance; qualities that are essential for wear parts that can withstand the rigors of the crushing process [5]. It has also the requisite toughness to undergo plastic deformation without cracking. Presently, the major challenge facing the quarrying industry in Nigeria is the high cost associated with worn-out wear plate that are predominantly made or manufactured from manganese steel.

Researchers have performed many studies to improve the wear resistance of Hadfield steels [6-9]. Microstructural phase transformation which is temperature dependent can be employed as a route for enhancing the wear characteristics of Hadfield Austenitic Manganese steel through the interplay of heat treatment. In the heat treatment process, the grain size in austenitic manganese steels before quenching is tremendously influenced by diffusive and diffusionless phase transformations, and precipitation [10]. The austenite grain size affects overall mechanical properties such as strength, hardness and ductility, hence its wear behaviour. Therefore, the influence of, solution heat treatment on the wear resistance of a typical Hadfield Austenitic Manganese use in quarrying industry was investigated.

2. Materials and methods

2.1 Material preparation

A sample representative from Hadfield Austenitic Manganese steel with composition of equivalent specification to NFMn128C was taken from a batch of 500 kg electric induction furnace melt to cast 4 bar of 200 × 11 × 11 mm to conduct the experiment. The charged materials used consist of 203 kg foundry returns, 220 kg low carbon steel, 10 kg of low carbon Ferro manganese, 65 kg high carbon Ferro manganese, 8 kg low carbon Ferrochromium, 2.19 kg Ferro silicon and 2.24 kg graphite powder respectively. The melting was carried out in a neutral lined refractory furnace. A digital pyrometer with disposable thermocouple tip was used for temperature measurement during melting and pouring. The molten metal was poured into an improvised CO_2 moulds in a mechanized foundry situated in Sango-Otta at the outskirt of Lagos, Nigeria.

2.2 Method

Patterns of dimension 202 × 11.2 × 11.2 mm were produced for the sand casting of the experiment. The sand used for the moulds was prepared by mixing dried silica sand, sodium silicate, water and bentonite in compliance to British standard. Thereafter, CO_2 gas was passed through the moulds for 80 seconds to cure the mould sand. To ensure correct mould identification, the moulds were labelled as A, B, C and D respectively. The charge make-up for the melt consist of Mn-Steel foundry returns (1.1 % C, 0.64 % Si, 12.4 % Mn, 1.2 % Cr, 0.006 % S, 0.005 % P, and 84.65 % Fe), Steel (0.20 % C, 0.35 % Si, 0.42 % Mn, 0.005 % S, 0.005 % P, and 99.02 % Fe), Low Carbon Ferro Manganese (0.23 % C, 75 % Mn), High Carbon Ferro Manganese (1.1 % C, 62 % Mn), Medium Carbon Ferro Chromium (0.5 % C, 67 % Cr), Ferro Silicon (0.02 % C, 70 % Si) and Graphite Powder (67 %).

The estimated charge make was calculated from Eq. 1.

$$\%(M) = \frac{(FeA/S)\%}{F_c} Q \tag{1}$$

In Eq. 1, M denotes melt, FeA denotes ferroalloy, S denotes scrap and F_c denotes furnace capacity. The furnace capacity represents the total charge in (kg), the Q represents the quantity of charge and % melt represent elemental concentration in the melt.

The standard compositions containing the lower and upper ranges of the specification for the melt of equivalent standard to NFMN128C is presented in Table 1.

Manganese as an element exhibits high oxidation tendency, therefore the manganese composition was deliberately calculated to be higher than the upper limit to ensure that the percentage of manganese is within the limit as a result of expected oxidation during holding of the molten metal in the furnace and de-slagging.

The raw materials as contained in the charge make-up in Table 2 for the melt were charged into the furnace in a particular order. The low carbon steel was charged first into a 500 kg medium frequency electric furnace lined with a neutral refractory material and allowed to melt completely. The selection of a neutral refractory was made deliberately to minimize furnace wall erosion as a result of slag attack. This was followed by the charging of the foundry returns, Ferro silicon, High carbon and Low carbon Ferro manganese and lastly graphite powder. The melting was completed after 94 minutes. The temperature of the molten bath was taken by a digital probe pyrometer with a disposable tip and recorded on an improvised daily furnace report. All procedures including personnel safety were observed during the melting and pouring operation.

The actual composition obtained after melting is presented in Table 3. The molten metal was poured at 1410 °C into the improvised CO_2 moulds, and allowed to solidify to room temperature after 12 h before they were knocked out and shot blasted. The 4-number castings were carefully fettled on a table grinding machine to the required dimensions 200 × 10 × 10 mm. During the grinding, care was taken to avoid work hardening on the surface of the casting.

Table 1 Chemical analysis result of melt of equivalent standard to NFMN128C

Specification	Elemental composition (%)					
	C	Si	Mn	Cr	S	P
Upper limit	1.30	0.80	14.00	1.50	0.005	0.005
Lower limit	1.00	0.60	12.00	1.00	0.005	0.005
Aim	1.28	0.70	14.34	1.52	0.004	0.005

Table 2 The Estimated charge make-up for Hadfield austenitic manganese steel

Description	Charge (kg)	Elemental composition (%)						
		C	Si	Mn	Cr	S	P	Fe
Foundry returns	203	0.437	0.25	4.84	0.47	0.002	0.002	bal
Steel	220	0.085	0.15	0.18	-	0.002	0.002	bal
Low Carbon Fe-Mn	10	0.004	-	1.46	-	-	-	-
High Carbon Fe-Mn	65	0.139	-	7.87	-	-	-	-
Ferro Chromium	8	0.007	-	-	1.05			-
Ferro Silicon	2.19	0.000	0.30	-	-	-	-	-
Graphite	2.24	0.555	-	-	-	-	-	-
Total	512	1.278	0.70	14.34	1.52	0.004	0.005	bal

Table 3 The compositional results obtained from bench top arc spectrometer

Elemental composition (%)					
C	Si	Mn	Cr	S	P
1.29	0.68	13.72	1.49	0.005	0.005

2.3 Heat treatment

The solution heat treatment process involves heating the sample at a particular heating rate. The choice of the heating rate depends on some factors such as the composition of the sample, shape of casting and the section thickness among other. For low carbon alloys and other alloy like manganese steels, their propensity to crack is extremely low, as such, the heating rate of 75 °C per hour. For high carbon specification or casting where warping of the sample may occur, a lower heating is adopted. The sample was heated to 1050 °C and held at this temperature for 24

min to allow the segregated carbides dissolve completely in solution in accordance to British standard. There after it was quenched quickly in a 500 l agitated water tank and allowed to cool room temperature.

2.4 Microstructural determination

A sample representative was taken from one as-cast and one heat treated cast bar. The surfaces were carefully prepared grinding on a tehrapol-31 machine, then polished with Allegrol with diamond suspension using a colloidal suspension of 0.04 μm silicon dioxide before they are etched in a solution of 100 ml alcohol and 3 ml HNO_3 acid at the Metallographic laboratory, Department of Mechanical Engineering. University of Ottawa, Ontario, Canada. An optical inverted Metallurgical microscope was used to study the microstructures. On the other hand, the morphology of the as-cast and heat treated samples were carried out using Scanning Electron Microscope (SEM) and Energy Dispersive Spectrum (EDS). The surface morphology of the worn out sample was also examined.

2.5 Micro-hardness value determination

Sample representatives were cut from the as-cast and heat treated bars for hardness testing. The samples were casted into resin mould, ground flat and polished. The hardness test was carried out on a Duramin-1 micro-hardness tester struers. An average of five measurements of hardness values was taken for as cast and heat treated manganese steel.

2.6 Wear test

Abrasive wear test were carried out on two prepared manganese steel castings (as-cast and heat treated) samples using pin-on-disc type equipment [11]. The wear test was carried out under varied load, and speed. After test each cycle of wear test, the mass of the worn out samples was measured with the aid of a digital weighing device with 0.001 mg accuracy to obtain the weight lost. Weight lost from the tests was used to calculate specific wear rate W, a parameter which defines wear severity from Eq. 1. From Eq. 1, V denotes volume loss of worn out sample, d_s denotes sliding distance, and L denotes applied load.

$$W = \frac{V}{d_s L} \tag{2}$$

The surface morphology of the worn out sample after the wear test was examined using optical microscope. The examined microstructure of the worn out, heat treated sample under high speed 4.72 m/s and 16 kN load is presented in Fig. 10. The surface morphology is characterized by needle like martensitic structure.

3. Results and discussion

3.1 Hardness and XRD test results

The result of the hardness test is presented in Table 4.

The indentation photo taken during the micro-hardness test is shown in Fig. 1(a) and Fig. 1(b) for heat treated and as-cast samples respectively. The solution heat treatment process inrease the hardness of the HAMnS sample. The increase in hardness might be due to fairly uniform distribution of the carbide phase in the austenite phase [2].

Table 4 Results of micro-hardness measurement

Description	Hardness, (HB)
As-cast Mn-steel	188
Heat treated Mn-steel	220

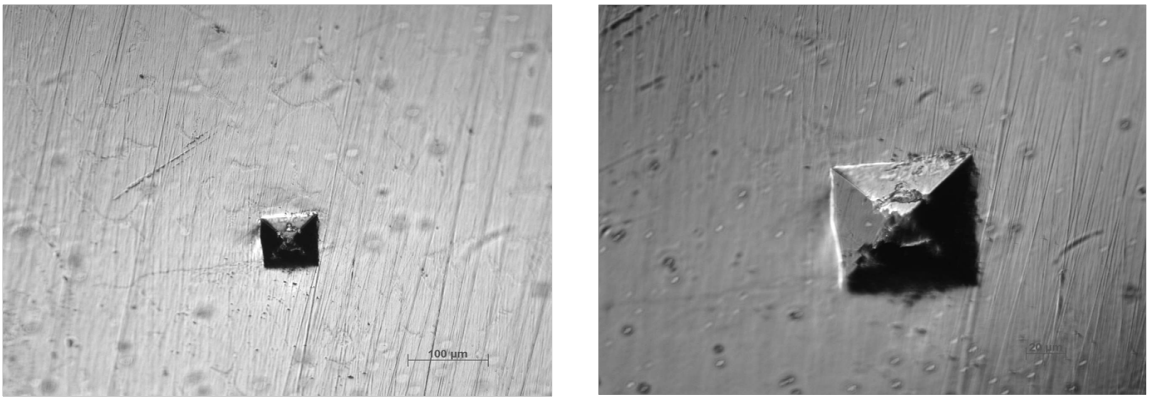

(a) (b)

Fig. 1 (a) Heat treated HAMnS indentation; (b) As-cast HAMnS indentation

The identified phases and compound formula from the XRD test for the manganese steel casting is presented in Table 5.

Table 5 Identified phases and their chemical formula

Score	Compound name	Chemical formula
38	Manganese	Mn
23	Carbon	C
21	Iron	Fe
21	Iron Silicon Carbide	Fe_9 Si $C_{0.4}$
14	Manganese Silicon Carbide	$Mn_{22.6}$ $Si_{5.4}$ C_4
12	Chromium Carbide	Cr_4 $C_{1.06}$
17	Manganese Silicon	Mn Si

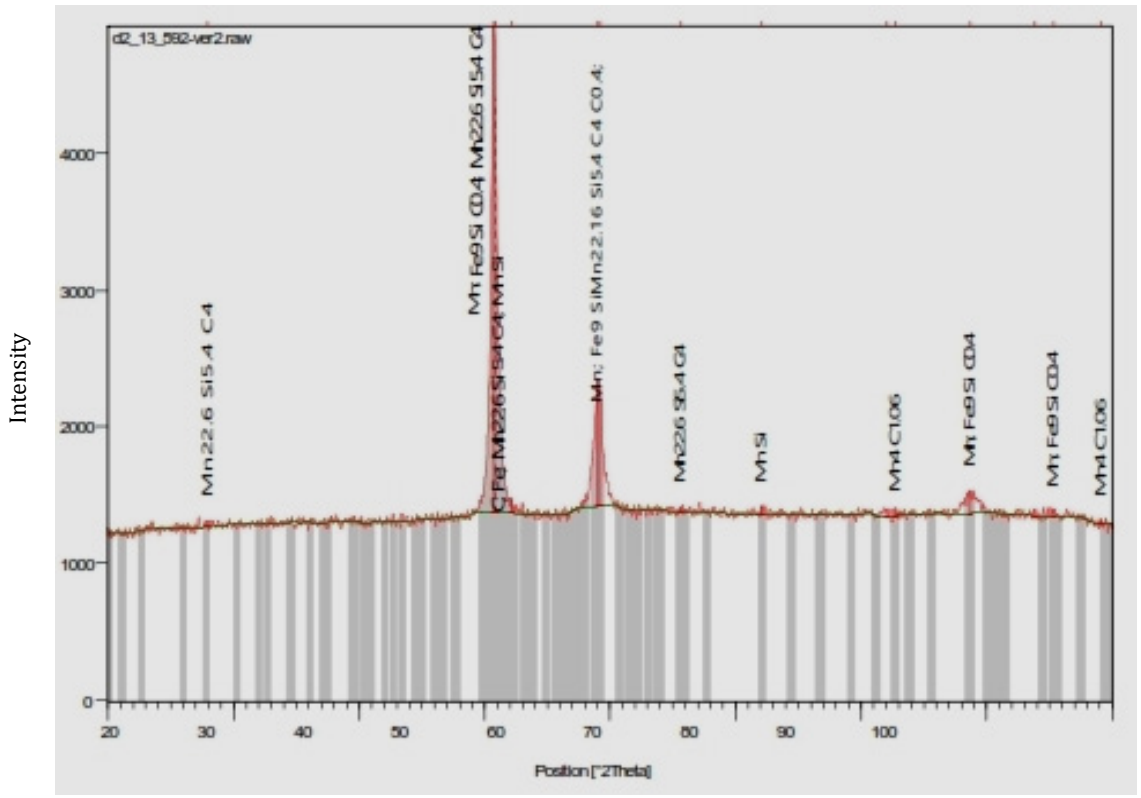

Fig. 2 The XRD profile of elemental segregation of manganese steel

3.2 Comparism between wear results and microstructure of as-cast manganese steel

Fig. 3 represents a graphical behaviour of the wear test results obtained for different load at the speed of 2.36 m/s for as-cast HAMnS. There is a general decrease in wear rate with increase in load. These phenomena may be attributable to increase interlocking of dislocation movement and to some extend work- hardening characteristics of the alloy. This same observed behaviour is replicated in a similar, but in a more pronounced manner at higher speed 4.72 m/s (Fig. 6). Hence, it can be infer that speed has significant effect on the wear behaviour of the manganese steel sample.

The observed non-uniformity in the wear profile curves of Fig. 1 and Fig. 2 can be attributed to the in-homogeneity of the as-cast HAMnS as revealed by the microstructure see Fig. 3. A non-uniform dispersion of the second phase (inter-metallic carbide) in the microstructure can be observed. The more heterogeneous the distribution of second phase particles, the more irregular the wear pattern of the as-cast HAMnS. This revealed that there is a strong relationship between distribution of second phase (Chromium carbide) and the wear nature of manganese steel.

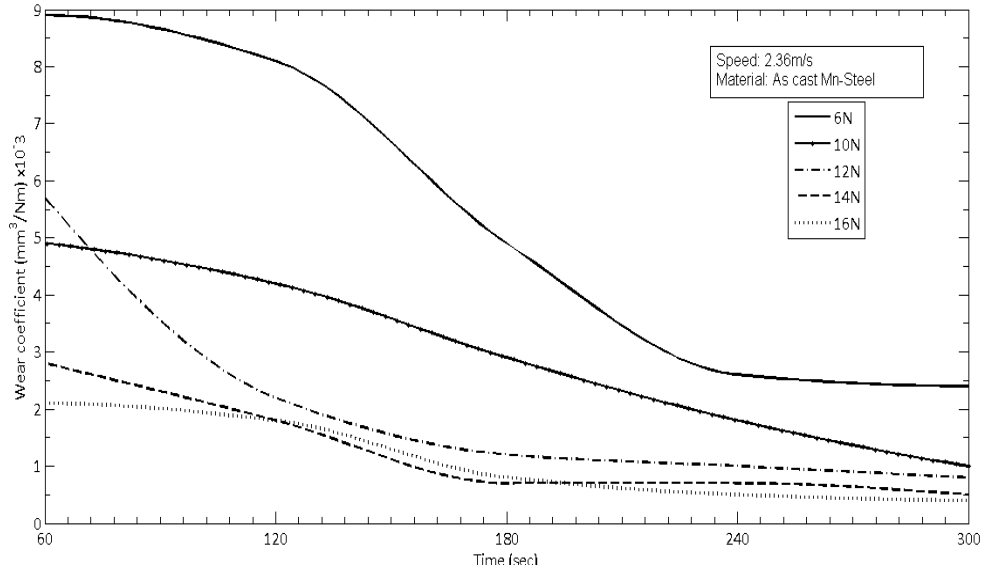

Fig. 3 Wear rate of as-cast HAMnS with time at 2.36 m/s and varying loads

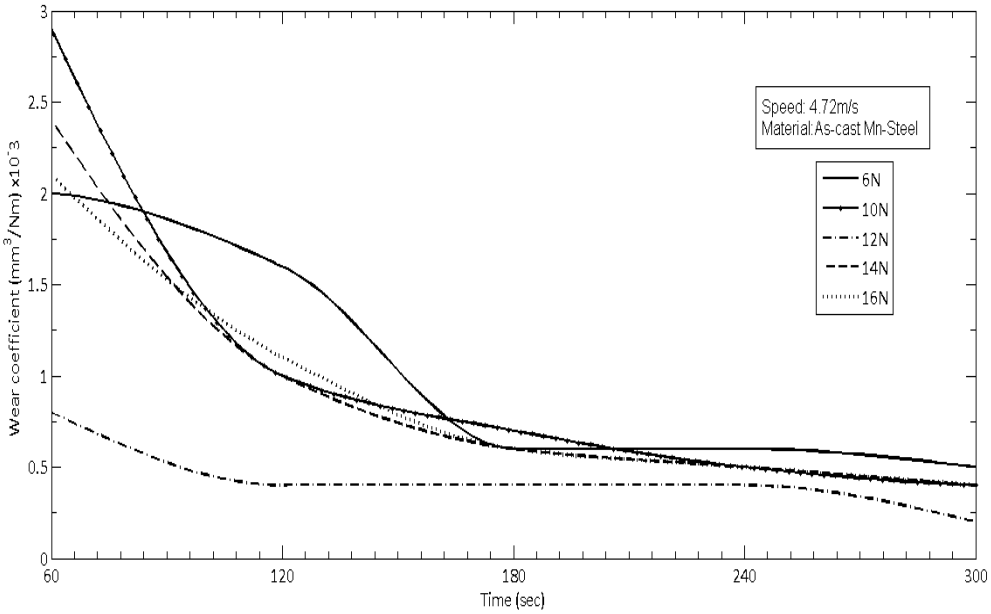

Fig. 4 Wear coefficient of as-cast HAMnS with time at 4.72 m/s for varying load

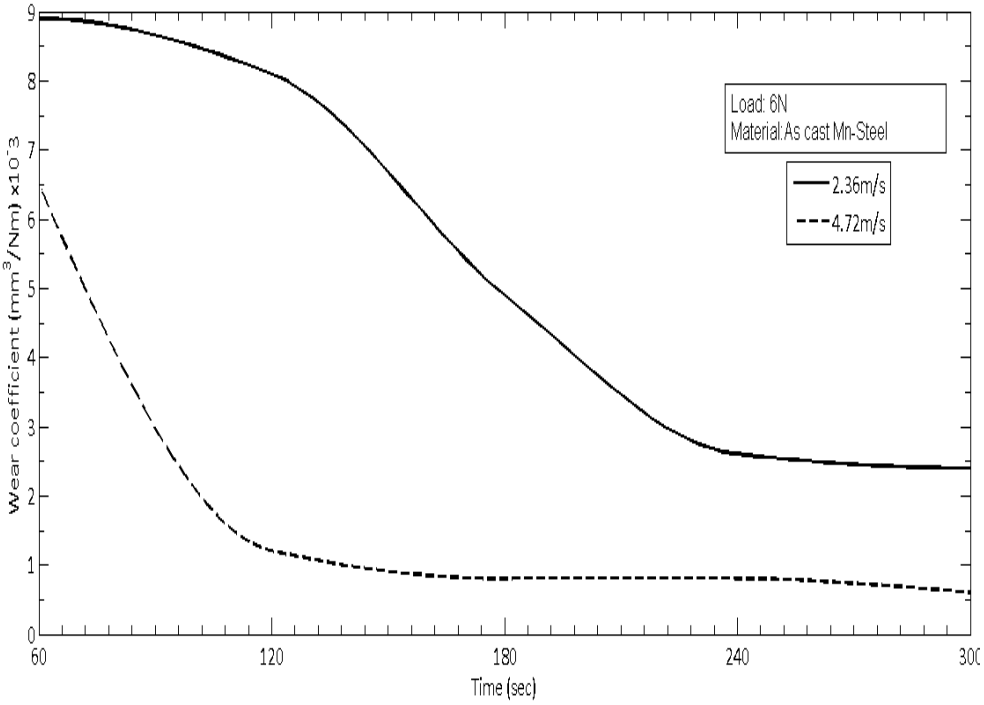

Fig. 5 Wear rate of As-cast HAMnS with time at 2.36 m/s and 4.72 m/s for load 6N

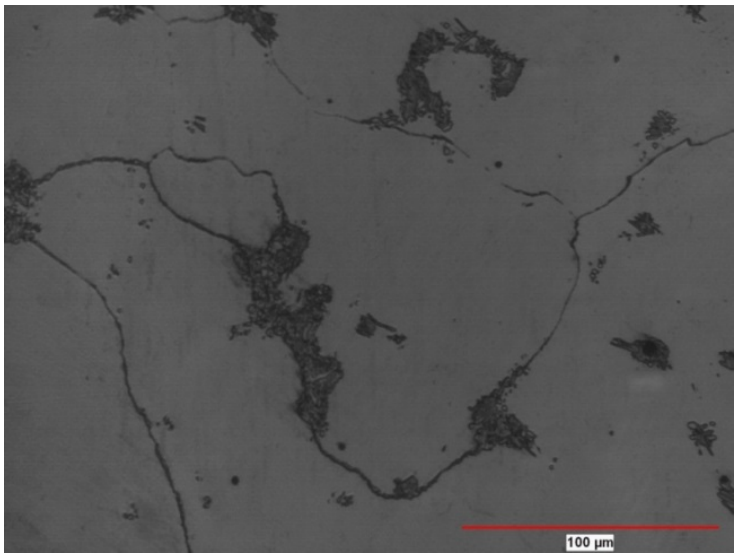

Fig. 6 The Optical micrograph of as-cast manganese steel showing significant heterogeneously dispersed chromium carbide within the austenite matrix of the microstructure at 100x

The wear rate of the HAMnS reduces significantly as the speed increases (Fig. 5). This further justifies the earlier assumption that speed has significant on the wear rate of the HAMnS sample. Increasing speed tends to improve the wear behaviour of the Mn-steel sample.

3.3 Comparison between wear results and microstructure of heat treated manganese steel

Fig. 7 shows smoother wear profile compared to Fig. 3. This can be attributed to the homogeneity of the heat treated manganese steel as revealed in the microstructure obtained after heat treatment (Fig. 9). The second phase particle (chromium carbide) as shown in Table 5 and Fig. 2 in the Xray-Diffraction result is uniformly dispersed with the austenite matrix. This development was attained after heat treatment (hardening) operation was carried out when the heterogene-

ously segregated second phase chromium carbide (Cr4C1.06) particle were dissolved in solution at 1050 °C, and quench in agitated water to trap the carbide within the matrix of the austenite.

A marked effect of load which became almost constant with increasing can also be observed. Time has no significant effect on the wear rate of Mn-steel sample. Similar to the as-cast sample, Fig. 8 shows that speed has significant effect on the wear behaviour of the heat treated sample.

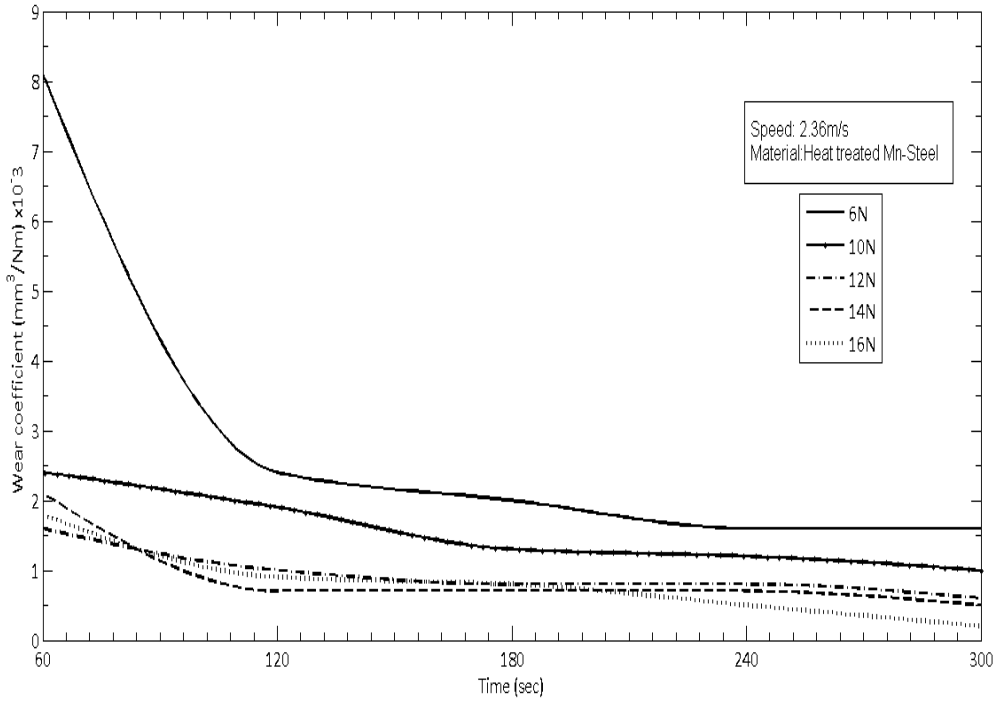

Fig. 7 Wear rate of Heat treated Mn-Steel with time at 2.36 m/s for varying load

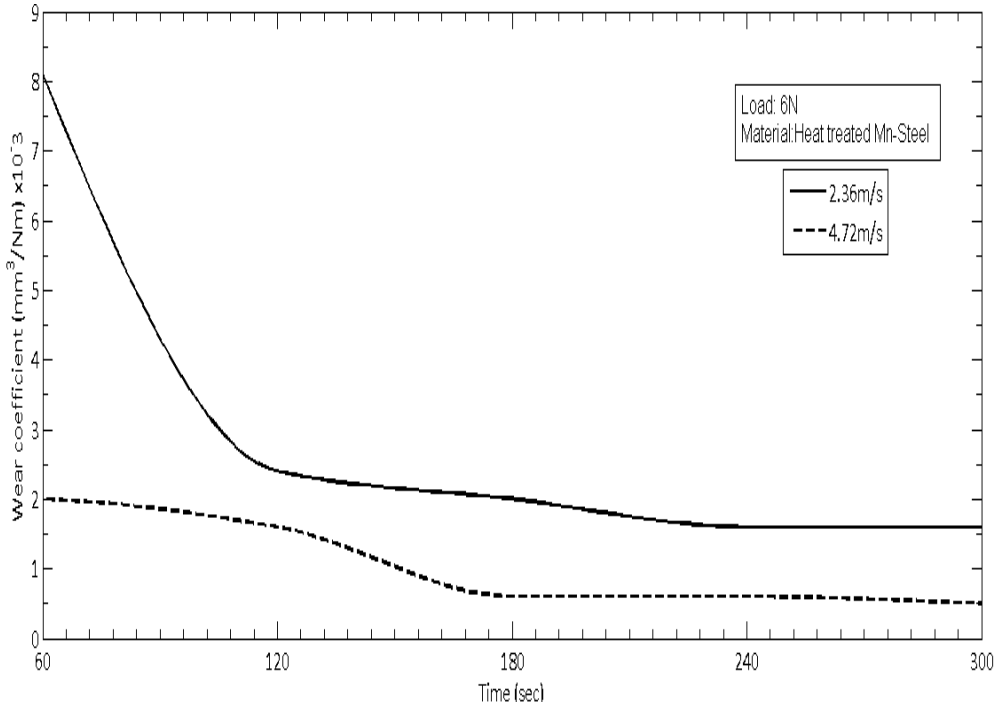

Fig. 8 Wear rate of Heat treated Mn-Steel with time at 2.36 m/s and 4.72 m/s, load 6N

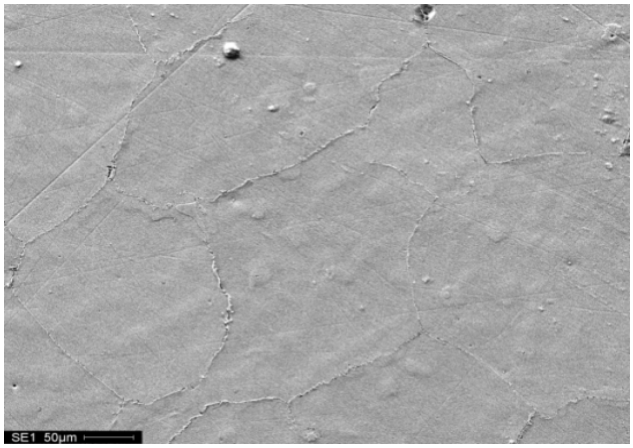

Fig. 9 The Optical micrograph (100x) of heat-treated manganese steel showing highly homogenous structure

The examined microstructure of the worn out, heat treated sample under high speed 4.72 m/s and 16 kN load is presented in Fig. 10. The surface morphology is characterized by needle like martensitic structure.

Fig. 10 Optical micrograph at 100x magnification of heat-treated manganese steel worn out- surface with evidence of high work hardenability after wear test

Fig. 11 shows the result of SEM and EDS analysis of the as-cast HAMnS. It was observed from Fig. 11 that the SEM micrograph is heterogamous in nature. This observation is similar to the Optical microstructure obtained in Fig. 6. The corresponding EDS corroborate the high degree of carbide segregation of Iron and Manganese.

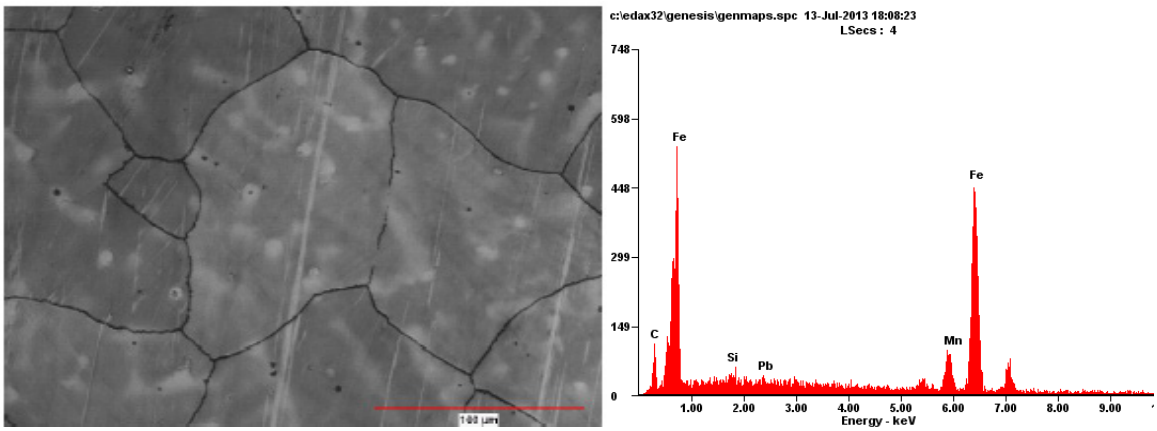

Fig. 11 The SEM micrograph and EDS of As-cast Manganese steel

The SEM micrograph with the corresponding EDS of the heat treated manganese steel is shown in Fig. 12. It was observed from the micrograph that the second phase chromium carbide particle is uniformly dispersed with the austenitic matrix. Again, this observation collaborated the earlier results obtained in Fig. 9 and agreed with the result of [5]. The degree of carbide segregation had been reduced considerably from the corresponding energy dispersion spectrum for heat treated HAMnS.

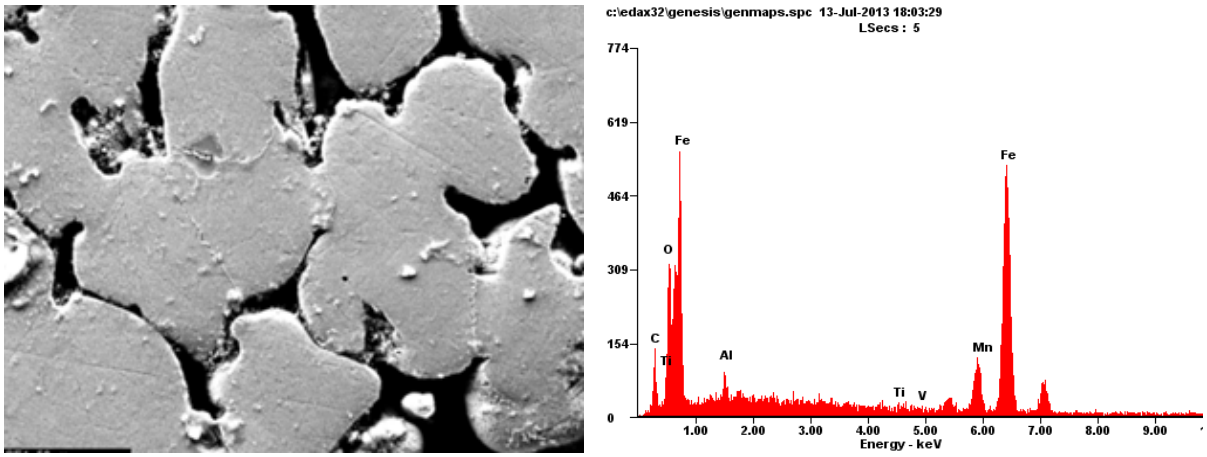

Fig. 12 The SEM and EDS micrograph of heat treated manganese steel

4. Conclusion

The wear behaviour of heat treated Hadfield austenitic manganese steel has been investigated. From the results of the investigations on the heat treated HAMnS the following conclusion were drawn.

1. The morphology and size of carbide phase has significant effect on the wear resistance of austenitic manganese steel.
2. The sliding speed-time interactions effect gave the most significant effect on the austenitic manganese steel
3. The solution heat treatment programme increased the wear resistance of the alloy steel under increasing load, speed and time.
4. The improved wear resistance of the manganese steel obtained was due to the formation of hard carbide phase within the matrix structure of austenitic manganese steel.
5. The wear behaviour of austenitic manganese steel can considerably be optimized by solution heat treatment and adequate quenching to redistribute the heterogeneous and segregated second phase chromium carbide to form a more homogenous and uniformly dispersed second-phase particle to enhance the wear resistance of the manganese steel.

Acknowledgement

The authors acknowledge the support from Nigerian Foundries Limited, Ilupeju Industrial Estate, Lagos for the exclusive use of her facilities to carry out this study. The authors would like to thank Dr. Micheal Nganbe, an associate Professor at the Department of Mechanical Engineering, University of Ottawa, Ontario Canada for his technical input and Dr. Mohammed Yadouzi a research fellow at the same Department who facilitated optical micrographs tests and interpretations.

References

[1] Mokken, A.H. (1969). The use of stainless steels in the mining industry; In: *Proceedings Symposium on Stainless steels*, Johannesburg, 83-102.

[2] Agunsoye, J.O., Talabi, S.I., Abiona, A.A. (2013). On the comparison of microstructure characteristics and mechanical properties of high chromium white iron with the hadfield austenitic manganese steel, *Journal of Minerals and Materials Characterization and Engineering*, Vol. 1, 24-28, doi: 10.4236/jmmce.2013.11005.

[3] Studnicki, A., Kilarski, J., Przybył, M., Suchoń, J., Bartocha, D. (2006). Wear resistance of chromium cast iron – research and application, *Journal of Achievements in Materials and Manufacturing Engineering*, Vol. 16, No. 1-2, 63-73.

[4] Agunsoye, J. (2009). *The Wear Characteristics of Austenitic Manganese Steel Casting*, PhD Thesis, University of Lagos, Nigeria.

[5] Balogun, S.A., Esezobor, D.E., Agunsoye, J.O. (2008). Effect of melting temperature on the wear characteristics of austenitic manganese steel, *Journal of Minerals and Materials Characterization and Engineering*, Vol. 7, No. 3, 277-289.

[6] Yan, W., Fang, L., Sun, K., Xu, Y. (2007). Effect of surface work hardening on wear behavior of Hadfield steel, *Materials Science and Engineering: A*, Vol. 460-461, 542-549, doi: 10.1016/j.msea.2007.02.094.

[7] Abbasi, M., Kheirandish, S., Kharrazi, Y., Hejazi, J. (2010). On the comparison of the abrasive wear behavior of aluminum alloyed and standard Hadfield steels, *Wear*, Vol. 268, No. 1-2, 202-207, doi: 10.1016/j.wear.2009.07.010.

[8] Bouaziz, O., Allain, S., Scott, C.P., Cugy, P., Barbier, D. (2011). High manganese austenitic twinning induced plasticity steels: A review of the microstructure properties relationships, *Current Opinion in Solid State and Materials Science*, Vol. 15, No. 4, 141-168, doi: 10.1016/j.cossms.2011.04.002.

[9] Aribo, S., Alaneme, K.K., Folorunso, D.O., Aramide, F.O. (2010). Effect of precipitation hardening on hardness and microstructure of austenitic manganese steel, *Journal of Minerals and Materials Characterization and Engineering*, Vol. 9, No. 2, 157-164.

[10] Xu, Y., Chen, Y., Xiong, J., Zhu, J. (2001). Mechanism of strain-induced nanocrystallization of Hadfield steel under high energy impact load, *Acta Metallurgica Sinica*, Vol. 37, 165-70.

[11] Agunsoye, J.O, Ochulor, E.F., Talabi, S.I., Olatunji, S. (2012). Effect of manganese additions and wear parameter on the tribological behaviour of NFGrey (8) cast iron, *Tribology in Industry*, Vol. 34, No. 4, 239-246.